Possibility of an Akhmediev breather decaying into solitons

Ch. Mahnke and F. Mitschke*
Universität Rostock, Institut für Physik, D-18051 Rostock, Germany
(Received 20 January 2012; published 13 March 2012)

We consider the process by which a constant or wide-pulse solution of the nonlinear Schrödinger equation can become converted into an ensemble of solitons by modulational instability. This process is generally believed to be one important step in the generation of supercontinuum in optical fibers. Starting from the Akhmediev breather solution we study the conversion by two methods: One is pulse shape-oriented and uses the soliton relation between width and peak power. The other is eigenvalue-oriented and uses results from scattering theory. It becomes clear that an evolution according to the unmodified nonlinear Schrödinger equation, even in the presence of noise, will not lead to the transformation into solitons. If one takes the Raman effect into account, however, a conversion to a soliton gas takes place.

DOI: 10.1103/PhysRevA.85.033808 PACS number(s): 42.81.Dp, 42.65.Tg

I. INTRODUCTION

Nonlinear propagation of light pulses in optical fibers is governed by the nonlinear Schrödinger equation [1] which is also relevant for nonlinear waves on liquid surfaces, in plasmas, in Bose-Einstein condensates, and so on. Currently the optics community is in intense discussion about the formation of optical supercontinuum [2], and in particular about rogue waves generated in the process [3]. All considered mechanisms for these waves share one property: Whether it is Raman shifting of the most intense solitons to the spectral fringe, collisions between solitons, or collisions of solitons with dispersive radiation. In any case, solitons must be generated first from the launch condition. When femtosecond pump pulses are used this is likely to happen through soliton fission; in all other cases (picosecond pulses or even cw pump) they supposedly arise from modulational instability [2]. A discussion of the instability has been put on a firmer footing since early reports about certain solutions of the nonlinear Schrödinger equation, the "Akhmediev breather" [4], have now found widespread attention.

The Generation of Trains of Soliton Pulses by Induced Modulation Instability in Optical Fibers was the title of a 1984 paper [5] in which conditions for the generation of a deeply modulated pulse train are discussed; however, the solitonic character of the individual peaks in the train was not discussed in any specific way. A few years later, the authors of Ref. [6] spoke of soliton-like structures atop a continuous background and the authors of Ref. [7] of a pulse train with a dc component. The authors of Refs. [8,9] discussed a pedestal which renders the pulse train unstable, thus preventing soliton train formation. As characteristics of solitons have now been well known for a long time, more precise statements can be made on just how the modulation instability relates to solitons. As there has been some confusion about this issue, we will discuss here whether the periodically modulated structure of modulational instability can be described in terms of solitons (i.e., more or less independent pulses).

The question is this: If the Akhmediev breather, a stable solution of the nonlinear Schrödinger equation, is the initial state and a set of fundamental solitons constitutes the final state how is the transition between the two triggered? Does a stochastic perturbation suffice? We will show that it does not. The nonlinear Schrödinger equation without additional terms cannot provide the conversion, but the Raman effect can.

II. PROPERTIES AND SYMMETRIES OF THE AKHMEDIEV BREATHER

It has been fully appreciated only recently that modulation instability can be described in the more general framework of the Akhmediev breather, obtained as early as 1986 [4]. It takes the form [10]

$$A(Z,T) = \sqrt{P_0}\frac{(1-4a)\cosh(bZ) + ib\sinh(bZ) + \sqrt{2a}\cos(\omega T)}{\sqrt{2a}\cos(\omega T) - \cosh(bZ)} \times \exp(iZ), \quad (1)$$

where normalized position $Z = z/L_{\mathrm{NL}}$, with distance z in meters. T is time in a comoving frame of reference. Power P_0 is measured in watts so that $(\gamma P_0)^{-1}$ is the "nonlinearity length" L_{NL} in meters. The nonlinearity parameter γ is measured in $\mathrm{W}^{-1}\mathrm{m}^{-1}$, typically in photonic crystal fiber (PCF) some 10^{-2} such units. Parameter a is from the interval $0 < a < 1/2$; parameter $b = \sqrt{8a - 16a^2}$ depends on a only and describes the gain. The modulation frequency is $\omega = \omega_c\sqrt{1-2a}$, and

$$\omega_{\mathrm{c}} = \pm\sqrt{\frac{4\gamma P_0}{|\beta_2|}} \quad (2)$$

is the highest frequency at which gain can occur. The dispersion parameter β_2 is measured in $\mathrm{s}^2\mathrm{m}^{-1}$, typically a few 10^{-27} such units. Note that b tends to zero for both $a \to 0$ and $a \to 1/2$. It peaks at ($a = 1/4$, $b = 1$) where the frequency becomes

$$\omega_{\max} = \pm\sqrt{\frac{2\gamma P_0}{|\beta_2|}} = \frac{\omega_{\mathrm{c}}}{\sqrt{2}}, \quad (3)$$

and the gain (perturbation growth rate) takes its maximum value of

$$g_{\max} = 2\gamma P_0. \quad (4)$$

*fedor.mitschke@uni-rostock.de

The solution to Eq. (1) evolves from a continuous wave with $|A(Z,T)|^2 = P_0$ at $Z \to -\infty$ through a compression and returns to $|A(Z,T)|^2 = P_0$ for $Z \to +\infty$ for any allowed a and all T. At finite Z the temporal modulation is periodic due to the ωT terms; the period is $T_{\mathrm{mod}} = 2\pi/\omega$. The maximally compressed case occurs at $Z = 0$. For later reference we mention specific values for the case $a = 1/4$. In each period the main peak has a power of $(1+\sqrt{2})^2\, P_0 \approx 5.83\, P_0$; a secondary peak of opposite field phase has peak power $(\sqrt{2}-1)^2\, P_0 \approx 0.17\, P_0$. The zeros in between appear as "dimples" in the power profile.

The Akhmediev breather quite generally has several symmetries. The periodicity with T_{mod} provides a time shift symmetry: at any given Z all peaks have the same shape and chirp. On account of the i sinh term there is an inversion symmetry about $Z = 0$: the pair of solutions at $\pm Z$ has identical power profiles and antisymmetric phase profiles. This implies zero chirp at $Z = 0$.

The spectrum pertaining to Eq. (1) is provided in Ref. [11]. Disregarding common constant factors it takes the form

$$\tilde{A}_C(Z) = 1 - \frac{ib\sinh bZ + (2-4a)\cosh bZ}{\sqrt{\cosh^2 bZ - 2a}} \tag{5}$$

for the carrier and

$$\tilde{A}_n(Z) = \frac{ib\sinh bZ + (2-4a)\cosh bZ}{\sqrt{\cosh^2 bZ - 2a}} \times \left[\frac{\cosh bZ - \sqrt{\cosh^2 bZ - 2a}}{\sqrt{2a}}\right]^{|n|} \tag{6}$$

for the nth sideband. Again there is an even real part and an odd imaginary part for both carrier and all sidebands.

As the continuous wave solution of the nonlinear Schrödinger equation is unstable, any perturbation (even if infinitely small) will give rise to a modulation. The initial cw field may be perturbed by quantum noise and by other, technical noise contributions. Fourier components of the perturbation that are close to the frequency of maximum gain [Eq. (3)] will grow fastest [Eq. (4)]. A purely random perturbation with white noise excites all frequencies equally; then modulation at the frequency of maximum gain will win out. Therefore the special case of $a = 1/4$, $b = 1$ has superior importance. We will now focus on this case.

The carrier phase evolves from $\phi_C(Z = -\infty) = -\pi/2$ through $\phi_C(Z = 0) = 0$ to $\phi_C(Z = +\infty) = +\pi/2$, whereas all sidebands have phases $\phi_n = \phi_C/2$ everywhere. Thus the phase difference $\phi_n - \phi_C$ evolves from $+\pi/4$ through 0 to $-\pi/4$. Note that quite generally a difference of $\pm\pi/2$ (sideband in quadrature with the carrier) pertains to pure phase modulation whereas a phase difference of 0 pertains to pure amplitude modulation. We see that in the Akhmediev breather there is a mixed modulation, with the exception of $Z = 0$ where the phase modulation vanishes, and the amplitude modulation takes its maximum expression.

We therefore arrive at the following intuitive way to understand the buildup and decay of the Akhmediev breather: Initially a mild phase modulation occurs on the continuous wave initial condition. In the temporal domain, tilted phases translate to velocities by virtue of the fiber's dispersion. Thus there are

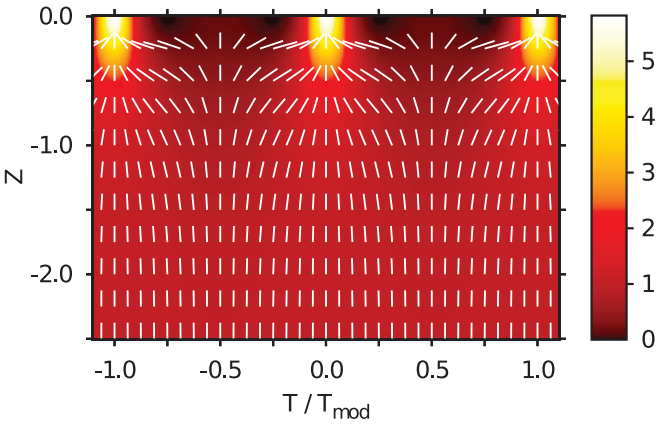

FIG. 1. (Color online) Evolution of Akhmediev breather ($a = 1/4$). Marker lines indicate transverse velocities due to phase dynamics. Color scale indicates P/P_0.

periodically alternating regions in which a velocity to the right and to the left exists. This causes power to be concentrated (focused) in some regions, and deconcentrated (defocused) in between. The concept is illustrated in Fig. 1 where the evolution from $-3 \leqslant Z \leqslant -0.1$ is shown for about two temporal periods of the breather; superimposed is a field of marker lines indicating the local phase slope (velocity). Intriguingly, the phase angle $\varphi(A(Z,0)) = \arctan\{\mathrm{Im}[A(Z,0)]/\mathrm{Re}[A(Z,0)]\} = \arctan(\sqrt{2}\sinh(Z))$ is very similar to and asymptotically the same (at least for $a = 1/4$) as the Gouy phase shift of a beam at a focus [12] for $Z \to \pm\infty$, $\varphi \to \pm\pi/2$. The Akhmediev breather can therefore be understood as a phenomenon of self-focusing and subsequent defocusing of a cw, complete with a resemblance of the Gouy phase shift.

We specifically consider a fiber into which light of average power P_0 is launched under conditions of anomalous dispersion. For Fig. 2 we launched the field given by Eq. (1) at $Z = -10$. At this position the cw background power is modulated almost sinusoidally, with extrema at $P_0 \pm 13 \times 10^{-5}$. This is a weak periodic perturbation, but still much larger than numerical noise. The corresponding approach has also been taken in experiments: the cw launch condition was artificially seeded with suitable coherent modulation in Ref. [5] and more

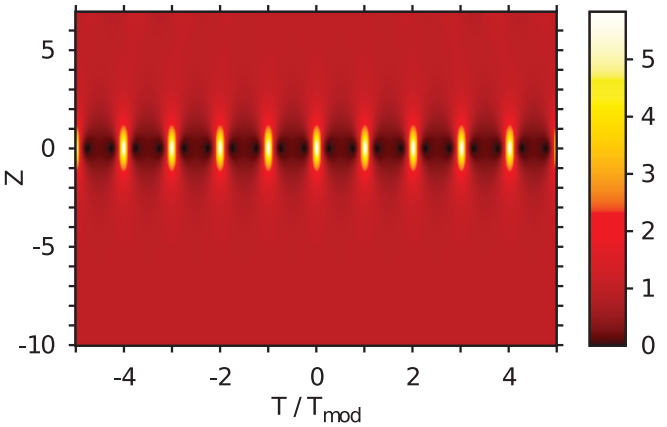

FIG. 2. (Color online) Evolution of Akhmediev breather started at $Z = -10$. Shading of color (gray) indicates P/P_0.

recently in Ref. [13]). Most prominent in Fig. 2 is the periodic comb of peaks at $Z = 0$. Between them one discerns the weak secondary peaks, and between the main and secondary peaks there are the "dimples."

III. SOLITON CONTENT ASSESSED FROM PULSE SHAPES

Clearly, the structure of maximum contrast is the most likely candidate for the generation of solitons. It was pointed out by the authors of Ref. [14] that the peaks have a "soliton number" close to unity. We rephrase this statement with better precision.

As is well known, soliton solutions of the nonlinear Schrödinger equation obey the constraint

$$\hat{P} T_0^2 = \frac{|\beta_2|}{\gamma}, \tag{7}$$

where $\hat{P}$ is the peak power and the width T_0 is taken from pulse center to the point where the argument of the sech function is unity. As the characteristic width of the Akhmediev breather solution we suggest taking the time from peak center ($T = 0$) to the point where the amplitude crosses the asymptotic value P_0. This is the most natural choice, as the Akhmediev breather has this asymptotic value for all allowed values of a. The width so defined is $T_{\mathrm{AB}} = T_{\mathrm{mod}}/8$ so that for $a = 1/4$

$$T_{\mathrm{AB}} = \frac{\pi}{4}\sqrt{\frac{|\beta_2|}{2\gamma P_0}}. \tag{8}$$

Remembering that $\hat{P} = (1+\sqrt{2})^2 P_0$, we obtain

$$\hat{P} T_{\mathrm{AB}}^2 = \frac{\pi^2(1+\sqrt{2})^2}{32}\frac{|\beta_2|}{\gamma} \approx 1.7976\frac{|\beta_2|}{\gamma}. \tag{9}$$

The numerical factor is, of course, strongly influenced by the choice of the width, but it is fair to concur with the authors of Ref. [14] that Eqs. (7) and (9) are quantitatively similar. However, there are subtle differences between the Akhmediev breather peak and solitons to be addressed. While at $Z = 0$ the phases of the Akhmediev breather are flat across the pulse, the smaller intermediate peaks have opposite phase. Phase jumps do not match well to solitons with their flat phases.

We are looking for a process that converts the train of peaks into individual solitons which can subsequently walk off like nearly independent particles. The Akhmediev breather pulse train, if harmonically seeded, is an entirely coherent structure. Therefore we look for a mechanism that can lift, or destroy, coherence. We therefore apply a random perturbation.

For Fig. 3 we combine the periodic perturbation described for Fig. 2 with an added noise of power standard deviation $\sigma_{\mathrm{ini}} = \sqrt{2} \times 10^{-4}$, somewhat larger than the periodic modulation. The noise was taken from a random number generator and transformed to give a Gaussian amplitude statistic with identically distributed phases throughout 2π.

Several relevant observations can be made from these data.

(1) Some teeth of the comb reach their maximum slightly sooner, others somewhat later than at $Z = 0$. The distribution of the Z positions of the maxima follows a Gaussian statistics centered on the deterministically expected value $Z = 0$.

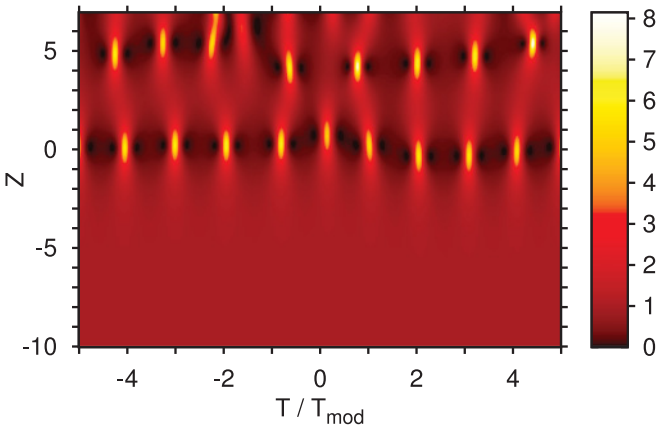

FIG. 3. (Color online) Evolution of Akhmediev breather as in Fig. 2, but here Gaussian noise with random phase was added at the starting position.

(2) There is also some variation in the peak powers. We checked that this distribution is centered on the deterministic value and has approximately Gaussian shape. Nonetheless the overall shape of the peaks remains closely similar to that of the analytical Akhmediev breather solution peak; the same conclusion was also drawn by the authors of Ref. [14]. We checked that the width of the peak power distribution σ_{peak} was approximately given by

$$\sigma_{\mathrm{peak}} = \sigma_{\mathrm{ini}} \exp(2\gamma P_0 L),$$

that is, it is consistent with the exponential growth of Eq. (4) over the relevant distance L, here ten units of Z.

(3) The phases at the maxima scatter about their deterministic value of π. Again, the distribution appears to be Gaussian.

(4) The periodicity of the comb at $Z = 0$ is still basically the same as in the noise-free case, but an enlargement of the neighborhoods of maxima reveals that some evolve with small transverse velocities (i.e., with a shift of their temporal position). We therefore evaluated the phase slope and curvature at the maxima; these also have a distribution approximately centered about the deterministic value, but it would take more data to confidently speak of a Gaussian distribution. The phase slope, of course, corresponds to a frequency offset; this together with the dispersion fully accounts for the observed velocities. The curvature corresponds to the chirp.

(5) A conspicuous difference of Fig. 3 from Fig. 2 is that beyond the compression a recurrence takes place at $Z \approx 15$. The reason is that the evolution of the Akhmediev breather sweeps out a heteroclinic orbit, so that depending on the fine detail of the initial starting condition the process may either ultimately return to a cw similar to the initial one, or repeat itself periodically. The latter situation has been described as a case of Fermi-Pasta-Ulam recurrence [15,16]. By adding noise, we perturbed the Akhmediev breather away from the heteroclinic orbit; the same was seen by others [10]. In mathematical terms, the Akhmediev breather solution is a special case of a more general solution expressed in terms of Jacobi elliptic functions [4,17]; an infinitesimal perturbation suffices to move the system away from this special case.

The transformation from an Akhmediev breather to solitons is also subject to an energy constraint. For reasons of energy

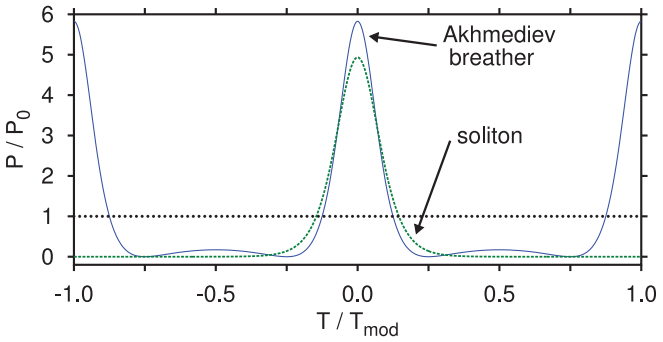

FIG. 4. (Color online) Temporal profile of the Akhmediev breather (dashed) and same-energy soliton (solid) in comparison. Power is in units of P_0, time in units of T_{mod}.

conservation the energy of an Akhmediev breather within one oscillation period is the same at $Z = 0$ and at any other position. Therefore the energy per period is

$$E_{\mathrm{AB}} = P_0 \frac{2\pi}{\omega} = \pi \sqrt{\frac{2|\beta_2|P_0}{\gamma}}. \tag{10}$$

To estimate the energy of a soliton generated from the breather we start with the oversimplifying assumption that this amount of energy gets incorporated completely into the soliton. Its energy would then be

$$E_{\mathrm{sol}} = 2\hat{P}T_0 = \pi \sqrt{\frac{2|\beta_2|P_0}{\gamma}}. \tag{11}$$

By using Eq. (7) one obtains

$$\frac{\hat{P}}{P_0} = \frac{\pi^2}{2} \approx 4.9348. \tag{12}$$

This is the highest peak power of a soliton generated from one period of the breather which is still consistent with energy conservation (see Fig. 4). A soliton matching the peak power of the breather, $(1+\sqrt{2})^2 P_0$, would be 18.1% higher and therefore 8.7% narrower than this, requiring 8.7% more energy (but the excess energy would have to come from somewhere). During propagation there might be an energy exchange with neighboring pulses, and in this sense energy conservation is not a strict requirement for each pulse. Surely, while some pulses may gain, others must lose.

Of course this upper bound is not realistic: While the breather at $Z = 0$ is unchirped, its shape involves zeros and sign reversals so that certainly there is dispersive radiation. This diminishes the energy available for the soliton. The energy contained in the main peak is

$$E_{\mathrm{peak}} = \int_{-T_{\mathrm{mod}}/4}^{+T_{\mathrm{mod}}/4} \left| \frac{\cos \omega T}{\cos \omega T - \sqrt{2}} \right|^2 dT = 0.95016\ E_{\mathrm{AB}}.$$

Similarly, by integrating between $T_{\mathrm{mod}}/4$ and $3T_{\mathrm{mod}}/4$ one obtains the energy in the secondary maximum, $E_{\mathrm{sec}} = 0.04984\ E_{\mathrm{AB}}$. One might argue, in a speculative manner, that only the difference between these two values, $E_{\mathrm{peak}} - E_{\mathrm{sec}} = 0.90032\ E_{\mathrm{AB}}$, can get incorporated into a soliton because to incorporate the opposite-phase contribution will invoke destructive interference. Remarkably, it will turn out below

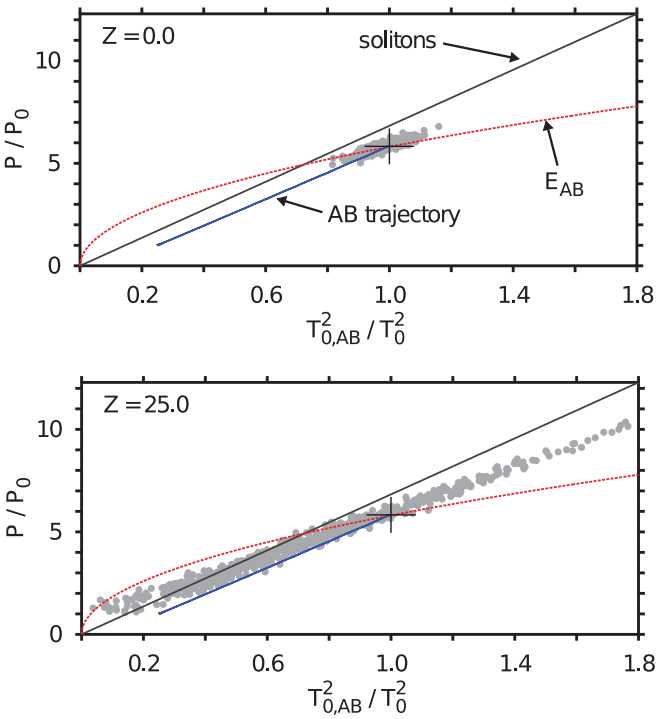

FIG. 5. (Color online) Diagrams of peak power $\hat{P}$ vs. the inverse square of temporal width T_0 of pulses. This format places all nonlinear Schrödinger equation solitons on the line labeled "solitons." Also shown are the trajectory traced out by the Akhmediev breather (the position of the cumulation point is highlighted by crosshairs) and the constant-energy contour at $E = E_{\mathrm{AB}}$. Initial conditions: Start at $Z = -10$ with weak noise ($\sigma_{\mathrm{ini}} = 10^{-6}$). Dots represent all identified maxima at $Z = 0$ (top) and $Z = 25$ (bottom).

that a very similar numerical value also arises from an entirely different argument.

We check the situation by numerical simulations. Data like those in Fig. 3 show clearly that the fully coherent structure of the Akhmediev breather breaks up soon after the position of maximum contrast. We see the recurrence which was described as "more complex" dynamics in Ref. [11]; it was pointed out there that neither loss, third-order dispersion, nor the Raman effect have an influence on its occurrence. We find that some pulses partially retain the "dimples" in the power profile, complete with phase jump, characteristic of the Akhmediev breather while other peaks have smooth shapes. It is obvious that the positions in both Z and T scatter considerably; not even the number of pulses is conserved. However, the system being nonlinear, there is a correlation between fluctuations of peak power and width. This is best assessed by representing a multitude of pulses in a $\hat{P}$-T_0^{-2} diagram as shown in Fig. 5. For this figure we identified the position of all maxima in the (Z, T) plane at $Z = 0 \pm 2$ (upper panel of Fig. 5) and at $Z = 25 \pm 2$ (lower panel of Fig. 5) The tolerance band was necessary because in the noisy case the Z positions of the peaks vary. For each identified maximum we then obtained $\hat{P}$ and T_0. While the former is straightforward, the latter requires a comment: In simulation data measures like the width at a certain percentage of the maximum often cannot be defined due to the close proximity of the next peak. We thus decided

to measure the curvature of each maximum, then calculate T_0 from that by using the conversion valid for sech^2 pulses.

Also shown in Fig. 5 is the trajectory of the Akhmediev breather (labeled as "AB trajectory"). It starts at $\hat{P} \approx P_0$ and minimal modulation, then contracts and traces out this trajectory in the process. The locus of the point of maximum contraction at $Z = 0$ is highlighted by crosshairs. Beyond that point the unperturbed breather traces out the same trajectory in reverse. To make the width of the Akhmediev breather and of solitons comparable for this figure, we again take the curvature at the peak (which here can be done analytically) and convert it to a pulse width in the same way as above. Finally, the constant energy contour of E_{AB} [Eq. (10)] is also shown for reference.

By virtue of Eq. (7), all unperturbed solitons of the nonlinear Schrödinger equation in a given fiber are expected to be represented by a point on the diagonal line with slope $|\beta_2|/\gamma$ labeled as "soliton line." Note that the reverse is not necessarily true: Pulses might fall onto that line and yet have a nonzero chirp, but then the pulse shape would keep evolving. It is obvious that the numerically obtained data points cluster near the Akhmediev breather culmination point initially, then spread out and form a long but thin cloud near the soliton line but not quite on it.

The intersection of the soliton line and the E_{AB} contour defines the maximum-energy soliton of Eq. (11). Clearly, a few peaks have increased in energy beyond this value. As mentioned above, that can happen by an exchange between neighboring pulses, but one peak's gain is its neighbor's loss.

We also checked the phases at all peak centers. They scatter over a 2π interval, but the distribution is not quite uniform. The pulses typically have linear phase slopes accounting for their velocities; with few exceptions they do not carry a large chirp. This indicates that in some sense they begin to resemble free, individual solitons. Will they eventually become completely free?

As the energy exchange between pulses proceeds slowly, no convergence to the soliton line is observed even when the propagation is followed for an extended distance ($Z = 80$). The core difficulty becomes apparent now.

The energy in the system is maintained. Analytically, the breather in Eq. (1) stretches to infinite time on either side; numerically we use periodic boundary conditions. Therefore the Schrödinger line cannot act as an attractor: pulses cannot converge toward it. Radiation shed by pulses remains in the system and will likely be reabsorbed by another pulse later on. Only an energy-losing mechanism would allow pure solitons to be approached. We therefore cannot expect that pulses evolve into clean solitons without some additional mechanism.

As a first test we modified the periodic boundary conditions of our computations such that there was some dissipation at the edges. This approximates realistic experimental situations. While a certain tendency of data points to get closer to the soliton line is observed, many data points still fail to join this trend, and further propagation does not seem to change this. It turns out that the recalcitrant cases tend to correspond to strongly chirped pulses. It is indeed difficult to see how dissipation could undo the chirp of a pulse. This makes it doubtful whether the stochastic perturbation can induce the transition to a set of solitons, but at this point a quite different method is required to resolve the issue.

IV. SOLITONS CONTENT ASSESSED FROM EIGENVALUES OF THE SCATTERING PROBLEM

To obtain information about the soliton content of some structure, the principal tool is the inverse scattering technique (IST) originally described for a different equation by Gardner *et al.* [18], improved by Lax [19], and first applied to the nonlinear Schrödinger equation by Zakharov and Shabat [20]. In its framework, solitons are described through certain discrete eigenvalues; in general, linear radiation is also produced which corresponds to the continuous part of the eigenvalue spectrum. It is of central importance to point out that IST relies on the integrability of the equation. We note in passing that for a more general class of systems, including those with dissipation, the recent technique of soliton-radiation beat analysis [21] can deliver equivalent results, and is advantageous in some circumstances.

In the present case we deal with a solution of an integrable equation, and so we decided to use the numerical IST-based technique introduced by the authors of Ref. [22] and known as direct scattering transform. It is a complication that the Akhmediev breather extends to infinity whereas the method presupposes data which decay to zero for $t \to \pm\infty$. We deal with this by considering a windowed Akhmediev breather. We multiply the expression in Eq. (1) with a window function which enforces a decay to zero on either side at finite width. Then we treat the window width as a variable, and attempt to extrapolate from finite to infinite width.

As a window function we initially experimented with a super-Gaussian, but it turns out that results are clearer when a rectangular window (value of 1 within width w, zero outside) is employed. We decided to center the window at $T = T_{\mathrm{mod}}/8$, at one of the zeros of the Akhmediev breather. The asymmetry of this choice avoids that with increasing window width two peaks enter the window at once. Using Eq. (1) at $Z = 0$ and this window all eigenvalues come out purely imaginary. When we refer to the eigenvalue below we mean the imaginary part which is indicative of a soliton's energy. Our results can be wrapped up as follows (compare Fig. 6).

As the window width is increased, a new pair of eigenvalues is born whenever the window's edge slices sufficiently deeply into a new peak; this occurs at half the peak's energy. One eigenvalue of each pair subsequently falls in value, the other

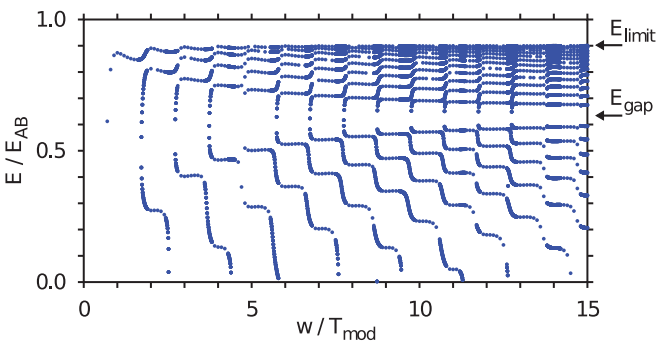

FIG. 6. (Color online) Position of eigenvalues as a function of window width. Also shown are the midgap position E_{gap} and the cumulation point of the eigenvalues above $E_{\mathrm{gap}}, E_{\mathrm{limit}}$ (see text). Window width is in units of the breather period.

rises. The rates of rise and fall are not uniform; when the window's edge begins to admit the secondary maxima of the Akhmediev breather's power profile (the parts with opposite phase), the trend is temporarily halted. This accounts for the conspicuous stair-like behavior. Near the energy level where eigenvalues are born there remains a gap between the multitude of rising eigenvalues and the multitude of falling eigenvalues.

The eigenvalues at each w fall into two groups. Above the gap there are as many as the window width measures in Akhmediev breather periods, except for edge effects. Below there are fewer because more than half of them have decayed to zero at any given width. The total number of eigenvalues diverges with $w \to \infty$, but normalization to the breather period provides an eigenvalue density which is finite. It is 1 (i.e., one per period) above the gap, and about 0.413 below so that the grand total approaches $(1.413 \pm 0.013)w$. The numerical factor is compatible with $\sqrt{2}$ within our computational precision, which may or may not be fortuitous.

The eigenvalues above the gap $E \geqslant (0.636 \pm 0.010)E_{\mathrm{AB}}$ arrange themselves in a remarkable pattern, reminiscent of a series of spectral lines near an accumulation point. The largest value E_1 is closest to the endpoint E_{limit}, and the others (E_n with $n = 2,3,\ldots,$) have distances growing quadratically like $E_n = E_{\mathrm{limit}} - n^2\Delta E$. Therefore no two eigenvalues are ever the same, nor do they ever cross. As the window width is increased, new eigenvalues appear and arrange themselves into this pattern. In the process ΔE shrinks and must tend to zero because a diverging number of eigenvalues is arranged within a finite interval. By fitting to the parabolic-distance arrangement we obtained the precise energy of the cumulation point as $E_{\mathrm{limit}} \approx (0.9003 \pm 0.0020)\, E_{\mathrm{AB}}$. No soliton has more energy than this value. To within numerical uncertainty, this value agrees with the heuristic value of $E_{\mathrm{peak}} - E_{\mathrm{sec}}$ above. It is tempting to think of this remarkable agreement as more than just fortuitous.

The extrapolation of the gap width to $w \to \infty$ (aided by plotting the same data on a $1/w$ inverse scale and extrapolation to zero, not shown) indicates that the gap shrinks to a point. Also, we find that $E_{\mathrm{limit}}/E_{\mathrm{gap}} = 1.416 \pm 0.025$ which is, again, close to $\sqrt{2}$.

In addition to the solitonic energies, the radiative contribution to the energy budget is calculated separately. When normalized to the window width, the sum of all contributions very closely (to within the numerical accuracy of 10^{-4}) approximates E_{AB}. The only exceptions occur at those w positions where new eigenvalues are born; apparently we do not immediately assess their energy correctly. The radiative part plays an ever smaller part as $w \to \infty$; apparently the radiation is an edge effect, not a volume effect.

A further characterization of this eigenvalue spectrum will be given elsewhere. Suffice it here to say that the characteristic feature in comparison to a similar spectrum obtained from a cw condition is the existence of the energy gap which is obviously linked to the periodicity of the potential.

As long as the propagation of the Akhmediev breather is described by the nonlinear Schrödinger equation without further terms the eigenvalues must be preserved. This fact has been exploited (e.g., for the suggestion of eigenvalue communication on grounds that eigenvalues are more robust than pulse shapes [23]). We find in our numerical simulations that both the real and imaginary parts of each eigenvalue are blurred into a small "uncertainty ellipse" when we add random noise. Similarly, numerical propagation introduces slight deviations from the original value. All these deviations can be attributed to numerical inaccuracies though. Certainly the number of eigenvalues is preserved in all cases we have seen.

The only possible conclusion from all this is the following. All breather peaks are identical, all solitons are different (and not even their total number matches). Obviously a one-to-one correspondence between the peaks of the Akhmediev breather and the solitons does not exist. The visible peaks must be the result of some nonobvious nonlinear superposition of the solitons described by the eigenvalues.

V. CONVERSION OF PULSE TRAIN TO SOLITONS BY RAMAN EFFECT

To create a number of solitons consistent with the number of peaks in the breather, it will therefore take a mechanism that can modify the eigenvalue spectrum. Linear loss can modify the number of eigenvalues through annihilation and even creation [24]. A truncated (i.e., windowed) Akhmediev breather, as one always has in real-world experiments, provides loss because power can leave the window at the edges. It is doubtful whether this is sufficient to generate free solitons because the loss continues and eventually must destroy all solitons.

A further possibility is the Raman effect, which, in practical terms, is always present anyway. The Raman effect is a scattering process that can transfer energy from some frequency component to another one of lower frequency (Stokes shift). The shape of the Raman gain spectrum in optical fibers was first studied by the authors or Ref. [25], and was later analyzed in more detail [26,27]. A consequence is that the energy of a pulse propagating in a fiber can be redistributed toward lower frequency [28]. The typical process is that pulses experience a continuous downshift in frequency, on account of the particular shape of the gain curve. This was discovered by the authors of Ref. [29] and analyzed by the authors of Refs. [30,31].

It was argued by the authors of Ref. [9] that the Raman effect acting on the pulse train generated by modulational instability can "separate the peaks from a pedestal" so that the pulses eventually behave like free particles. We tested this proposition; it will turn out that it is basically correct. As an initial condition we used Eq. (1) at $Z = 0$, then studied its propagation in a split-step Fourier simulation based on a nonlinear Schrödinger equation with an added Raman term. For the latter we employ the widely used formulation from Ref. [32].

In the presence of the Raman effect, all eigenvalues above the gap acquire a real part indicative of a frequency shift toward lower frequencies (a "red shift"). In contrast, all eigenvalues below the gap experienced a shift in the opposite direction ("blue shift"). This is shown in Fig. 7 where the evolution of the eigenvalues of a truncated Akhmediev breather was followed for the propagation from $Z = 0$ to $Z = 1$ (i.e., over one nonlinear length). Somewhat counter to expectation, not the

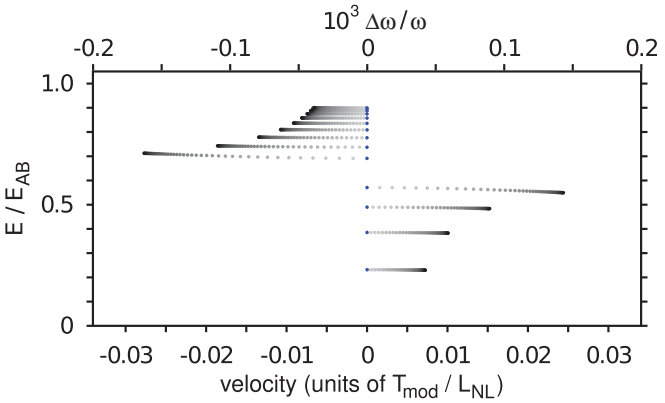

FIG. 7. (Color online) Eigenvalues shifting red and blue. Data from propagation starting with the analytic AB solution at $Z = 0$, calculated form a NLSE with added Raman term, and evaluated with direct scattering transform.

most energetic eigenvalues undergo the strongest change, but the ones closest to the gap. This is a further argument against identifying the Akhmediev breather peaks with solitons. The phenomenon of opposite-direction frequency shift is visible in a very mild form in higher-order soliton fission [33], where it appears like a recoil effect, but Fig. 7 seems to suggest a dispersion curve at a gap resonance so that one may attribute the shifts seen here to the periodicity of the structure.

The frequency shifts translate into velocities, and so both subsets of eigenvalues lose their temporal overlap after some propagation distance. The resulting structure is shown in Fig. 8. The set of red-shifted eigenvalues corresponds to a group of pulses with nonequal peak powers and widths, arrayed in a not very regular pattern. The power and width of each peak closely obey the soliton condition Eq. (7) (see Fig. 9). The pulse phases are scattered almost uniformly through a 2π interval. Next-neighbor phase differences do not seem to exhibit any particular correlations. The first derivative of the phase is indicative of the velocity; the values found reflect the direction of the trajectories in Fig. 8. The second derivative indicates the chirp; all these pulses have very small chirp. Assessing these findings together, one can interpret the situation in only one way: A set

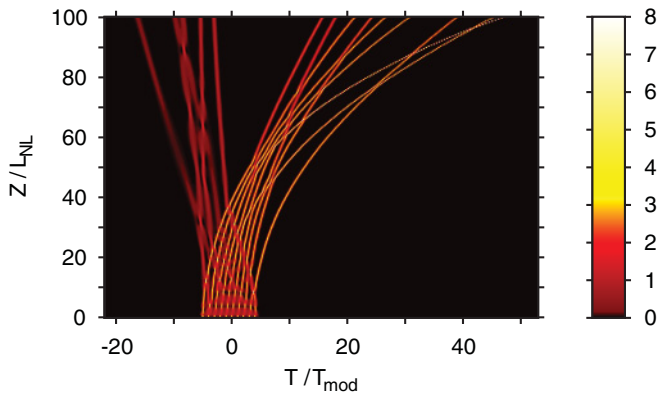

FIG. 8. (Color online) A truncated Akhmediev breather, subject to Raman shift, splits into a red-shifting soliton gas and a set of blue-shifting weaker solitonic pulses.

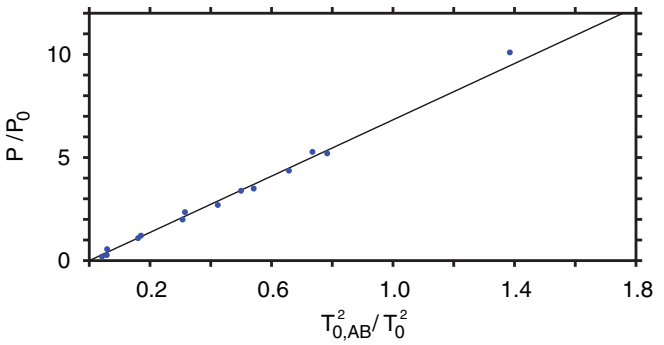

FIG. 9. (Color online) Soliton relation Eq. (7) tested on the final state after Raman shift. All data points are close to the soliton condition; they also have minimal chirp (not shown).

of solitons has been created; within the limits set by their rather close proximity, they behave as nearly independent entities.

The blue-shifted eigenvalues constitute a separate group of pulses with much lower power, but they also closely fulfill the soliton constraint Eq. (7) (see the leftmost data points in Fig. 9). This group was interpreted as a pedestal by the authors of Ref. [9]. They have much smaller velocities, but may have a somewhat larger chirp than pulses from the other group. All peaks from both groups are evaluated for their compliance with the soliton constraint in Fig. 9, and it is obvious that they now are in accord to within numerical accuracy.

To corroborate our interpretation that in the Raman-shifted case each pulse may indeed be interpreted as a soliton, we compare the numerically derived values of energy and velocity for each peak with the locus of eigenvalues in the complex plane, as shown in Fig. 10. The number of eigenvalues corresponds to the number of peaks; each eigenvalue can be uniquely attributed to one peak, and the numerical agreement is satisfactory. In the energy balance, all solitonic energies from the eigenvalues add up to about 0.99; if the radiative part is also included, the balance exceeds unity by 2.7×10^{-3} which we attribute to the cumulation of numerical round-off errors.

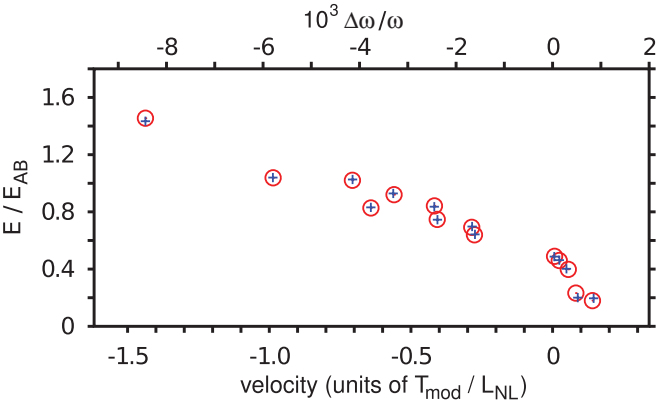

FIG. 10. (Color online) Interpretation of eigenvalues of the Raman-shifted pulses in the complex plane scaled as to represent energy and velocity units. Data correspond to Fig. 8 at $Z = 100L_{NL}$. Crosses: Locus of eigenvalues obtained with direct scattering transform. Circles: Energy and velocity values obtained directly from the numerically calculated peaks. The close agreement shows that each peak uniquely corresponds to one eigenvalue.

All told, a truncated Akhmediev breather with n peaks initially contains $\approx 1.41n$ solitons in a nonobvious way. By the Raman shift eventually a group of n individual solitons is formed, while the remaining solitons are initially blue-shifted. The solitons in either subset do not sit on a regular grid. The high-power solitons in particular move about nearly independently of each other except when they come quite close to a neighbor. Therefore it seems fitting to call this group a soliton gas.

VI. CONCLUSION

We have discussed the similarities between the Akhmediev breather and solitons, and have analyzed the breather's scattering eigenvalues. This involved finding eigenvalues of an infinite system.

Several authors [5–7,34] have suggested schemes to exploit modulational instability for the generation of trains of pulses, also in the presence of the Raman effect [35]. Typically it was not mentioned that the train of pulse will decay again, so the fiber must be cut at the point of maximum expression. It has sometimes been conjectured, and more often tacitly assumed, that the train of peaks arising from modulational instability breaks up easily into an ensemble of individual solitons. It turns out that this is oversimplified; any conclusions based thereupon about soliton robustness of the generated structures would be flawed.

The conversion of a modulation instability-induced structure into a train of solitons cannot happen without factors beyond the standard nonlinear Schrödinger equation. There is no direct correspondence between the solitons as identified through their eigenvalues and the peaks of the Akhmediev breather structure. Noise weakens the coherence between Akhmediev breather peaks, but by itself does not change the number of eigenvalues. Therefore it cannot set the individual pulses free to evolve into solitons.

Modifications of the pulse train generation from modulational instability have been discussed, such as an incorporation into a laser resonator [36,37]. In such a case the gain dynamics may well provide the means to stabilize the pulse train. The conclusion presented by the authors of Ref. [9] that a conversion to solitons can happen through the Raman effect now finds its justification and factual base in the behavior of the scattering eigenvalues. With respect to the applications of modulational instability alluded to in the Introduction, namely structure generation in the context of supercontinuum generation and possibly rogue wave studies, the Raman effect is always present in any realistic setting. Therefore we expect that in that context indeed a group of individual solitons will be generated, and with the present contribution we clarify the mechanism.

ACKNOWLEDGMENTS

FM enjoyed fruitful discussions with Ulf Peschel (Erlangen). The authors gratefully acknowledge financial support by Deutsche Forschungsgemeinschaft.

[1] G. P. Agrawal, *Nonlinear Fiber Optics*, 4th ed., (Academic Press, New York, 2007).
[2] *Supercontinuum Generation in Optical Fibers*, edited by J. M. Dudley and J. R. Taylor, (Cambridge University Press, Cambridge, England, 2010).
[3] D. R. Solli, C. Ropers, P. Koonath, and B. Jalali, Nature (London) **450**, 1054 (2007).
[4] N. N. Akhmediev and V. I. Korneev, Theor. Math. Phys. **69**, 1089 (1986).
[5] A. Hasegawa, Opt. Lett. **9**, 288 (1984).
[6] E. J. Greer, D. M. Patrick, P. G. J. Wigley, and J. R. Taylor, El. Lett. **25**, 1246 (1989).
[7] S. Sudo, H. Itoh, K. Okamoto, and K. Kubodera, Appl. Phys. Lett. **54**, 993 (1989).
[8] E. M. Dianov, P. V. Mamyshev, A. M. Prokhorov, and S. V. Chernikov, Opt. Lett. **14**, 1008 (1989).
[9] P. V. Mamyshev, S. V. Chernikov, E. M. Dianov, and A. M. Prokhorov, Opt. Lett. **15**, 1365 (1990).
[10] N. Akhmediev, A. Ankiewicz, J. M. Soto-Crespo, and J. M. Dudley, Phys. Lett. A **375**, 775 (2011).
[11] K. Hammani, B. Wetzel, B. Kibler, J. Fatome, C. Finot, G. Millot, N. Akhmediev, and J. M. Dudley, Opt. Lett. **36**, 2140 (2011).
[12] S. Feng and H. G. Winful, Opt. Lett. **26**, 485 (2001).
[13] B. Kibler, J. Fatome, C. Finot, G. Millot, F. Dias, G. Genty, N. Akhmediev, and J. M. Dudley, Nat. Phys. **6**, 790 (2010).
[14] J. M. Dudley, G. Genty, F. Dias, B. Kibler, and N. Akhmediev, Opt. Express **17**, 21497 (2009).
[15] E. Fermi, J. Pasta, and S. Ulam, Studies of Nonlinear problems. Los Alamos Report LA-1940, 1955. Reprinted in E. Fermi, *Collected Papers Vol. II*, edited by E. Segrè, (University of Chicago Press, Chicago, 1965), p. 978.
[16] N. N. Akhmediev, Nature (London) **413**, 267 (2001).
[17] N. N. Akhmediev, V. M. Eleonskii, and N. E. Kulagin, Theor. Math. Phys. **72**, 809 (1988).
[18] C. S. Gardner, J. M. Greene, M. D. Kruskal, and R. M. Miura, Phys. Rev. Lett. **19**, 1095 (1967).
[19] P. D. Lax, Commun. Pure Appl. Math. **21**, 467 (1968).
[20] V. E. Zakharov and A. B. Shabat, Sov. Phys. JETP **34**, 62 (1971).
[21] M. Böhm and F. Mitschke, Phys. Rev. E **73**, 066615 (2006); Appl. Phys. B **86**, 407 (2007); Phys. Rev. A **76**, 063822 (2007).
[22] G. Boffeta and A. R. Osborne, J. Comput. Phys. **102**, 252 (1992).
[23] A. Hasegawa and T. Nyu, J. Lightwave Technol. **11**, 395 (1993).
[24] J. E. Prilepsky and S. A. Derevyanko, Phys. Rev. E **75**, 036616 (2007).
[25] R. H. Stolen, C. Lee, and R. K. Jain, J. Opt. Soc. Am. B **1**, 652 (1984).
[26] R. H. Stolen, J. P. Gordon, W. J. Tomlinson, and H. A. Haus, J. Opt. Soc. Am. B **6**, 1159 (1989).
[27] R. H. Stolen and W. J. Tomlinson, J. Opt. Soc. Am. B **9**, 565 (1992).

[28] E. M. Dianov, A. Y. Karasik, P. V. Mamyshev, A. M. Prokhorov, V. N. Serkin, M. F. Stel'makh, and A. A. Fomichev, JETP Lett. **41**, 294 (1985).
[29] F. M. Mitschke and L. F. Mollenauer, Opt. Lett. **11**, 659 (1986).
[30] J. P. Gordon, Opt. Lett. **11**, 662 (1986).
[31] V. N. Serkin, T. L. Belayeva, G. H. Corro, and M. Agüero Granados, Quantum Electron. **33**, 325 (2003).
[32] K. J. Blow and D. Wood, IEEE J. Quantum Electron. **25**, 2665 (1989).
[33] K. Tai, A. Hasegawa, and N. Bekki, Opt. Lett. **13**, 392 (1988).
[34] A. S. Gouveia-Neto, M. E. Faldon, A. S. B. Sombra, P. G. J. Wigley, and J. R. Taylor, Opt. Lett. **13**, 901 (1988).
[35] A. S. Gouveia-Neto, M. E. Faldon, and J. R. Taylor, Opt. Commun. **69**, 325 (1989).
[36] M. Nakazawa, K. Suzuki, and H. A. Haus, IEEE J. Quant. El. **25**, 2036 (1989).
[37] P. Franco, F. Fontana, I. Christiani, M. Midrio, and M. Romagnoli, Opt. Lett. **20**, 2009 (1995).